Med Discoveries
An open access journal of science and medicine

Article Type: Research Article
Volume 5, Issue 2
Received: Jan 21, 2026
Accepted: Feb 18, 2026
Published Online: Feb 25, 2026

Preclinical Evaluation of a Fluorine-18 Labeled Transthyretin Small Interfering RNA Transfection Platform as an Imaging Probe for Liver Fibrosis

Li Dai[1]; Qi-Yong Guo[3]; Fan-Lei Kong[2,3]*; Yan-Li Shi[1]*

[1]Department of Stomatology, Shandong Provincial Hospital Affiliated to Shandong First Medical School, Jinan 250000, China.

[2]Department of Radiology, Qilu Hospital of Shandong University, Jinan 250000, China.

[3]Shengjing Hospital Affiliated to China Medical University, Shenyang 110004, China.

***Corresponding Author:** Fan-Lei Kong & Yan-Li Shi*

Tel: +86 18518052427 & +86 15168888963; Email: Kongfanlei-md@126.com & jnsyl@163.com

Abstract

Introduction: It has been reported that dysregulated Transthyretin (TTR) transcript and decreased protein expression during fibrotic progression. Therefore, TTR gene is expected to become a target for hepatic fibrosis monitoring. The study aims to prepare and evaluate a fluorine-18-labeled transthyretin siRNA molecular probe targeting TTR mRNA for PET imaging of liver fibrosis preclinically.

Methods: The molecular probe was a penetrating peptide complexed with TTR-siRNA by noncovalent bonds. The targeting specificity of this probe for TTR mRNA was evaluated in cellular experiments including fluorescence imaging and western blots. [^{18}F] was used to label the TTR-siRNA probe using benzaldehyde as a carrier to prepare the [^{18}F] TTR-siRNA positron probe. [^{18}F] TTR-siRNA targeting to TTR mRNA was confirmed by comparing the Standardized Uptake Value (SUV) of the probe in normal rats (S0 stage) regularly expressing the TTR gene and liver fibrosis (S4-stage) rats with low TTR gene expression.

Results: Cellular fluorescence experiments demonstrated that uptake of the TTR-siRNA molecular probe was pronounced at 80 min and peaked at 12 h, confirming TTR mRNA targeting. The western blots result well supported the fluorescence results, illustrating a significant reduced TTR protein in liver cells treated with TTR-siRNA probe, as compared with that in the negative control and blank cell groups. Positron emission tomography-computed tomography (PET/CT) imaging with animals showed that SUVmax and SUVmean of [^{18}F] TTR-siRNA molecular probe were significantly higher in normal rats (S0) than in liver fibrosis rats (S4) at 80 min after injection ($P<0.05$). Differences in accumulation of the [^{18}F] TTR-siRNA molecular probe in the liver of normal and liver fibrosis rats were in line with the results of cell and immunohistochemistry experiments.

Conclusion: [^{18}F] TTR-siRNA molecular probe was prepared and evaluated preclinically. The probe targeted TTR mRNA in the hepatic cytoplasm and hold potency for noninvasive targeted gene imaging in liver fibrosis assessment.

Keywords: Transthyretin; Liver fibrosis; Small interfering RNA (siRNA); Molecular imaging; Positron Emission Computed Tomography (PET).

Introduction

Liver fibrosis is a common pathological stage as chronic liver disease develops into cirrhosis, which ultimately leads to hepatic dysfunction, portal hypertension and hepatocellular carcinoma [1-3]. The status of liver fibrosis has a certain reversibility and efforts to inhibit, alleviate or even reverse liver fibrosis could greatly improve the prognosis of liver diseases [4]. Liver biopsy is the gold standard for diagnosis and staging of liver fibrosis [5,6]. However, the clinical practice of liver biopsy has limitations due to its invasiveness, material selection, patient compliance and poor reproducibility. Noninvasive imaging assessment of the degree of liver fibrosis is clinically important.

Citation: Dai L, Guo QY, Kong FL, Shi YL. Preclinical Evaluation of a Fluorine-18 Labeled Transthyretin Small Interfering RNA Transfection Platform as an Imaging Probe for Liver Fibrosis. Med Discoveries. 2026; 5(2): 1288.

Traditional imaging methods including optics, ultrasound, Computed Tomography (CT), and Magnetic Resonance Imaging (MRI) [5-8], provide information on liver tissue morphology, stiffness, and perfusion. In particular, magnetic resonance elastography shows a high correlation with semiquantitative liver fibrosis staging. However, most approaches do not directly reflect liver fibrosis stages and are affected by factors such as parenchymal inflammation, hepatic vascular congestion, steatosis or portal hypertension, which interfere with the accuracy of identifying the S0, S1, and S2 stages of liver fibrosis. Establishing a precise pathological model of liver fibrosis and achieving noninvasive, targeted imaging are essential for improving liver fibrosis diagnosis, precise therapeutic effects, and early prevention of liver cancer.

Numerous molecular imaging methods including MRI, PET/CT, single photon emission computed tomography, and fluorescent imaging [9,10], have been used to directly monitor biological processes of liver fibrosis *in vivo* and to assess the extent of liver fibrosis at the cellular and molecular levels. Most molecular probes target and bind to specific molecules in activated macrophages, extracellular matrices, or activated hepatic stellate cells. These molecules include collagen [11], fibrin-fibronectin complexes [12,13], translocator protein [14], integrin receptor αvβ3 [7,15], Axiology coprotein Receptor (ASGPR) [16], desmin and vimentin [17]. These molecules tend to be highly upregulated in the process of liver fibrosis. Molecular probes using biomarkers including polypeptides, aptamers, or small chemical ligands are typically developed for different imaging modalities.

Oligonucleotide-based therapy is an actively developing area of drug development for treating various gene-specific diseases with unique specificity and high efficiency. Small interfering RNA (siRNA) is a promising and attractive platform to construct gene therapeutic tools applicable to liver fibrosis [18-21]. SiRNAs are generally double stranded RNA with 21-23 nucleotides which could generate cascading effects causing sequence-specific messenger RNA (mRNA) cleavage or translation repression [22]. Various non-viral transfection vectors are available for cytoplasmic targeting of siRNA, such as cationic polymers, lipids, or cell-penetrating-peptides-based vectors. In addition, synthetic siRNAs also have the potential for chemical modification to enhance their stability, specificity, and safety, and for bulk production. The combination of siRNA-based RNA interference technology and nuclear medicine has created a new and noninvasive gene imaging diagnostic method, which can reveal genes of interest *in vivo* through nucleic acid hybridization [23-26]. Imaging of genes closely related to liver fibrosis progression will accurately provide important information on the pathological progression of liver fibrosis.

Transthyretin (TTR), also known as pre-albumin, is a tetramer of four identical subunits. TTR is produced by hepatocytes and the choroid plexus. Its main function is as a transporter protein that participates in the transport of thyroxine and retinol. The use of TTR inhibitors stabilizes the TTR structure and prevents its decomposition, leading to tissue fibrosis [27]. Caillat F et al. [28] reported that TTR gene is dysregulated between S0 and S4 fibrosis stages, with a down-regulation during S0 to S1, up-regulation during S1 to S2-S3 followed by a significant down-regulation during F3 to F4 progression. In addition, the gradual decrease serum level of TTR protein during fibrosis progression also indicate TTR to be a novel serological marker. Therefore, the TTR gene or protein is expected to be a potential marker for liver fibrosis assessment.

In this study (Figure 1), an siRNA targeting a specific sequence of TTR mRNA was selected as a biomarker for liver fibrosis. A transfection vector based on a polypeptide was used for effective transfection of the siRNA. The fluorine-18 labeled molecular probe was prepared using fluorine-18 ([18F])-labeled benzaldehyde as an intermediate to evaluate the TTR-targeting behavior *in vivo*. We evaluated the targeting effect of the molecular probe to the TTR gene using cellular experiments and determined the targeting capability of the prepared ^{18}F-labeled molecular probe to TTR mRNA *in vivo* using PET/CT imaging in a rat model. The goal was to understand the feasibility of the TTR-siRNA-based probe for liver fibrosis imaging and diagnosis.

Materials and Methods

Materials and reagents: The N-TER™ Nanoparticle siRNA Transfection System (N-TER, Cat. N2913) was purchased from Sigma-Aldrich (USA). TTR siRNA, Cyanine-3-labeled TTR siRNA, negative control siRNA, and Cyanine-3-labeled negative control siRNA were obtained from Jima Gene Co., Ltd. (Suzhou, China), and their sequences are listed in (Table 1). Normal rat liver BRL3A cells were purchased from North Natron Biotechnology Research Institute (China), and Male Wistar rats weighing approximately 300 g were acquired from the Benxi Experimental Base of Sheng Jing Hospital of China Medical University. DMEM culture medium, penicillin, and streptomycin were obtained from Kaiji Biotechnology Co., Ltd (Jiangsu, China). Fetal bovine serum and trypsin were from Gibco Life technologies (USA). Rabbit anti-rat TTR primary antibodies were obtained from Origene (USA). HRP-labeled goat anti-rabbit secondary antibodies were obtained from Solarbio Biotechnology Co., Ltd (Beijing, China), and 4-formyl-N, N, N-trimethylaniline triflate was acquired from Huayi Technology Co., Ltd (Jiangsu, China).

Cell culture and establishment of liver fibrosis in rats: Normal rat liver BRL3A cells were cultured using DMEM medium containing 10% fetal bovine serum and 80 U/ml penicillin, 0.08 mg/ml streptomycin in a 37°C, 5% CO_2 incubator. At about 90% confluence, cells were digested with trypsin for sub-culturing.

Male Wistar rats weighing about 300 g from the Benxi Experimental Base of Sheng Jing Hospital of China Medical University were used. The rats were kept in a clean grade animal room in Sheng Jing Hospital of China Medical University at 23±1°C. All experimental protocols were approved by The Animal Care and Use committee of Sheng Jing Hospital of China Medical University. All experiments were conducted in accordance with the Animal Guidelines of Sheng Jing Hospital of China Medical University. To establish a liver fibrosis model, rats were intraperitoneally injected with 300 mg/kg thioacetamide solution twice a week. Rats in the control group were intraperitoneally injected with an equal volume of normal saline twice a week for the same period.

Preparation of TTR-siRNA molecular probe targeting to TTR mRNA: TTR siRNA (Suzhou Jima Gene Co., Ltd., Table 1) and DEPC Water (Suzhou Jima Gene Co., Ltd.) were used to prepare a 5 μM TTR siRNA solution. The Nanoparticle siRNA Transfection System (N-TER) (Sigma-Aldrich) was used. Prepared TTR siRNA solution was mixed with N-TER polypeptide solution and incubated at room temperature for 15-20 min to noncovalently bind TTR siRNA to N-TER polypeptide to form a stock solution of TTR-siRNA molecular probe (denoted N-TTR-siRNA) at 650 nM. The N-TER-assisted transfection negative control siRNA probe N-NC-siRNA was prepared through the same procedure used for N-TTR-siRNA. The stock solution was diluted according to

the transfection concentration needs.

Fluorescence imaging experiments to evaluate time-dependent cellular uptake of the TTR-siRNA molecular probe in vitro: The cyanine-3-labeled molecular probes Cy3-N-TTR-siRNA and Cy3-N-NC-siRNA were prepared according to the same protocol as N-TTR-siRNA and N-NC-siRNA preparation by substituting each siRNA by cyanine-3-labeld ones. Rat BRL3A cells were seeded in six-well plates at 1.2×10^5 per well and cultured in a 37°C, 5% CO_2 incubator for 12 h. Then, culture media in six-well plates were aspirated and 3 mL 40 nM Cy3-N-TTR-siRNA and Cy3-N-NC-siRNA in the culture media were added for the TTR and NC groups before incubation in a 37°C, 5% CO_2 incubator. The Blank Control (BC) group was treated with the same volume of siRNA buffer. Cells were subjected to fluorescence imaging using a fluorescence microscope at 80 min, 4 h, 8 h, 12 h, 24 h, 48 h, and 72 h post incubation. Fluorescence intensity-time curves were quantified using ImageJ software to calculate the ratio of total fluorescence intensity in the cytoplasm of fluorescence images to cell number as a quantitative parameter. In brief, each fluorescence image was converted into 8-bit type and adjusted on the basis of the same threshold. The integrated intensity was measured and normalized to the cell number in each fluorescence image to obtain the quantified ratio at different time points for comparison.

Targeting of TTR-siRNA molecular probe to hepatocyte TTR gene by western blots: To assess the TTR gene-silencing effect of the TTR-siRNA molecular probe, cell samples from the TTR, NC and BC groups were obtained using the method in the last section, by substituting the corresponding siRNA-treated groups with non-fluorescently labeled siRNA and incubating for 48 h. Media were then aspirated and cells were washed 2-3 times with PBS. An appropriate volume of RIPA buffer (with protease inhibitor added a few minutes before use) was added to culture plates for 3-5 min before scraping cells with a cell scraper. Harvested cells were added to 1.5 ml centrifuge tubes. Collected cells were lysed on an ice bath for 30 min. Supernatants were collected by 12,000 rpm centrifugation at 4°C for 10 min and protein concentration was determined by the BCA method. An equal amount of protein sample was taken from each group and denatured with SDS loading buffer and boiling for 15 min. Samples were used for then subjected to conventional SDS-PAGE gel electrophoresis. Proteins were transferred to PVDF membranes using a wet membrane transferring method. Blocking used 5% skim milk powder at room temperature for 1 h. Rabbit anti-rat TTR primary antibody (Origene, USA) was used for incubation overnight at 4°C. After 3 TBST washes, HRP-labeled goat anti-rabbit secondary antibody (Beijing Solarbio Biotechnology Co., Ltd.) was used for incubations for 30 min at room temperature. ECL chemiluminescence coloring solution was used for signal development. β-actin was the housekeeping protein.

^{18}F positron nuclides labeling for the [^{18}F] TTR-siRNA molecular probe: The [^{18}F] TTR-siRNA molecular probe synthesis process is in (Figure 2). ^{18}F ions produced by a cyclotron were transferred to TRACER lab FX fn (GE Corporation, USA). After QMA treatment with ^{18}F ions, 15 mg K222 (Kryptofix 2.2.2, dissolved in 1 ml of acetonitrile) and 3 mg potassium carbonate (K_2CO_3) dissolved in 0.5 ml water were evaporated to dryness in a TRACER lab FX fn reaction flask. In 500 µl DMSO, 5 mg 4-formyl-N, N, N-trimethylaniline triflate was dissolved and added to the reaction flask for heating at 110°C for 10 min. Temperature was lowered to 35°C and product was added to HPLC eluent and separated by HPLC (40% alcohol, flow rate 8 ml/min, UV 254 nm) to yield 4-18F-fluorobenzaldehyde ([^{18}F] FB).

Such benzaldehyde containing aromatic group was used to further react with the amino group at the end of N-TER to form stable Schiff base. The 4-18F-fluorobenzaldehyde (0.5 ml in alcohol) and 0.5 ml of N-TER were dissolved in 1 mL 0.5 M sodium acetate (NaOAc) buffer (pH 4.5), and heated at 70°C for 10 min. The mixture was separated by HPLC (40% alcohol, flow rate 8 ml/min, UV 254 nm) to yield [18F] FB-N-TER. The final product had an uncorrected radiochemical yield of 25±5%.

Prepared TTR siRNA solution was mixed with [^{18}F] FB-N-TER and incubated at room temperature for 15-20 min to obtain the final [^{18}F] FB-N-TER-TTR siRNA molecular probe (shortened as [^{18}F] TTR-siRNA).

In vivo PET/CT imaging of rats: Rats in the healthy groups and liver fibrosis model groups at the fourth week after thioacetamide solution treatment were selected for PET/CT imaging. Rats were fasted and not supplied with water 6 h before imaging. Before imaging, 10% chloral hydrate was injected 0.3 ml/100 g intraperitoneally for anesthesia. Supine position scans were used for imaging. Rats in the liver fibrosis model and control groups were injected with 0.5 mCi [^{18}F] TTR-siRNA probes into tail veins. Dynamic scanning was implemented with VIP scanning mode of PET/CT instrument (GE Discovery Elite). The PET scan layer thickness was 3.75 mm and CT scan parameters were 80 kV, 50 mA, and layer thickness 3.75 mm. At the end of CT scans, PET dynamic scans were performed continuously for 60 min and regular scans were performed at the 80th minute. Acquired images were deconvolved by Sharp IR+VUE Point HD image reconstruction technology, and the OSEM iterative reconstruction method. Image processing was performed by GE AW4.5 and Xeleris 3.0 workstations. Three-dimensional PET and CT and fusion images of the two with cross-sectional, sagittal, and coronal sections and radioactivity-time curves of rat livers were constructed. Under guidance of CT images, large blood vessels were avoided on PET images from routine scanning at the 80th min. Two 50-mm^2 regions of interest were drawn in each of the left, middle and right liver lobes from the liver fibrosis model and healthy groups. Corresponding SUVmax, SUVmean and SUVmin were obtained.

Pathology and immunohistochemistry: All rats were sacrificed immediately after the end of imaging scans. After 14 days fixation in 10% formaldehyde, routine Hematoxylin-Eosin (HE) staining, sirius red staining and TTR molecular pathological staining were performed. Scheuer scoring system was used for liver fibrosis staging. TTR expression was quantified using immunohistochemistry.

Statistical analysis

Data analysis was performed in SPSS 23 software. The Kolmogorov-Smirnov method was used to test the normal distribution of measurement data as SUVmax, SUVmean and SUVmin. If data points did not meet normal distribution, median values (upper and lower quartiles) were used. The liver fibrosis model and healthy groups were compared with Mann-Whitney U tests. Differences were statistically significant at $P<0.05$.

Results

Time-dependency of cellular uptake of TTR-siRNA molecular probes: Fluorescence experiments demonstrated that the molecular probe prepared by noncovalent binding of

N-TER and TTR siRNA was synthesized and achieved intracellular transfection (Figures 3A and 3C). When the N-TER was used as the carrier into cells, the fluorescence intensity of TTR siRNA in cells was higher than for the same concentration of NC siRNA (Figures 3A and 3B). Fluorescence intensity versus time curves (Figure 3D) showed that fluorescently labeled TTR siRNA with N-TER as the vector entered cells after 80 min and intracellular accumulation of TTR siRNA peaked at 12 h, gradually declining with time.

TTR-siRNA molecular probe targeting for the TTR gene at the cellular level: After incubation for 48 hours with reagents in the three groups (blank cell group, TTR-siRNA-, and NC-siNRA-probe-treated cell groups), cells were collected for western blot analysis (Figure 4). As compared with that in the NC and blank cell groups, TTR protein in liver cells treated with the TTR-siRNA molecular probe was obviously reduced.

[^{18}F] TTR-siRNA molecular probe for PET/CT scan in rats: Pathological results confirmed that rats in the healthy group were in fibrotic S0 stage (Figures 5A and 5B) and rats in the liver-fibrosis model group were in fibrotic S4 stage (Figure 5D and 5E). Immunohistochemistry showed that expression of TTR in livers of rats from the healthy group was higher than in rats from the liver-fibrosis model group (Figures 5C and 5F). Radioactivity-time curves in (Figure 6) showed decreasing liver radioactivity over time for both of healthy and fibrotic rats. However, the discrepancy of radioactivity between the two groups was appearing since 24th minute and higher tracer uptake of healthy rat liver became significant at the end of scanning (80th minute after injection). Statistical analysis (Table 2) showed that the SUVmax and SUVmean of rats from the healthy group were higher than rats in the liver-fibrosis model group and differences were significant ($^{a}P<0.05$). There was no significant difference in SUVmin among rats from the two groups ($^{b}P>0.05$).

Table 1: Sequences of TTR siRNA and negative control siRNA.

Name	Sequence
TTR siRNA sense	5'-mCAGmUGmUmUmCmUmUGmC-mUmCmUAmUAAdTdT-3'
TTR siRNA anti-sense	5'-UmUAmUAGAGmCAAGAAmCACUG-dTdT-3'
Negative control siRNA sense	5'-UUCUCCGAACGUGUCACGUTT-3'
Negative control siRNA antisense	5'-ACGUGACACGUUCGGAGAATT-3'

m, corresponding base 2' hydroxy methylation modification; Cy3 labeled the end of the sense strand in fluorescence experiments.
Abbreviation: TTR: Transthyretin; siRNA: small interfering RNA.

Table 2: Comparison of [^{18}F] TTR-siRNA molecular probe uptake parameters for liver fibrosis model and control (healthy rat) groups at the 80th minutes after probe injection.

	SUV max	SUV mean	SUV min
Liver fibrosis model group*	1.865 (1.770,2.063)	1.585 (1.295,1.823)	1.190 (0.089,1.563)
Control group*	2.660 (2.435,3.020)	2.300 (1.703,2.403)	1.520 (1.200,2.050)
Z value	-2.722	-2.246	-1.121
P value	0.004	0.026	0.310

*Statistics by median value of upper and lower quartile.

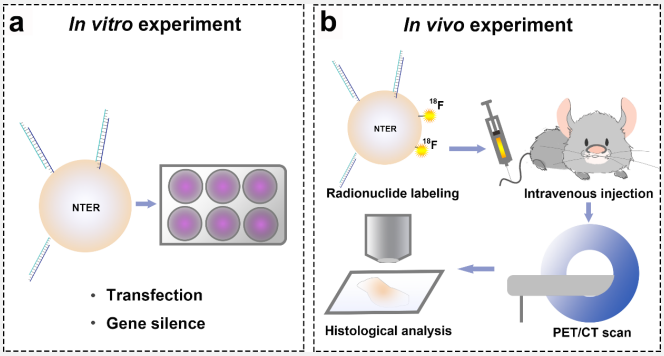

Figure 1: Experimental schemes. **(A)** SiRNA targeting a specific sequence of TTR mRNA as a biomarker for liver fibrosis was complexed with a peptide-based transfection vector (N-TER) to form a TTR-siRNA molecular probe for siRNA transfection. Targeting of the TTR gene by the TTR-siRNA molecular probe was analyzed by cellular experiments. **(B)** ^{18}F labeling of the molecular probe body constituted the PET molecular probe [^{18}F] TTR-siRNA. Molecular probe targeting of TTR mRNA for *in vivo* imaging was evaluated by PET/CT imaging and immunohistochemistry in the rat model.
Abbreviation: TTR: Transthyretin; siRNA: Small Interfering RNA.

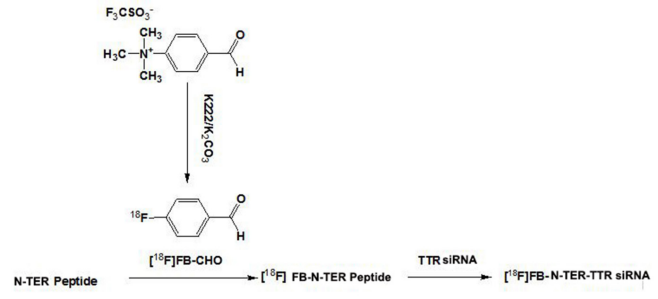

Figure 2: Schematic illustration of [^{18}F] TTR-siRNA molecular probe preparation. ^{18}F labeling of N-TER by 4-[^{18}F]-fluor benzaldehyde. TTR siRNA noncovalent bonded with N-TER to form a positron siRNA-based molecular probe, [^{18}F] FB-N-TER-TTR siRNA molecular probe (shortened as [^{18}F] TTR-siRNA), that targeting TTR mRNA.
Abbreviation: TTR: transthyretin; siRNA: small interfering RNA; FB: fluor benzaldehyde.

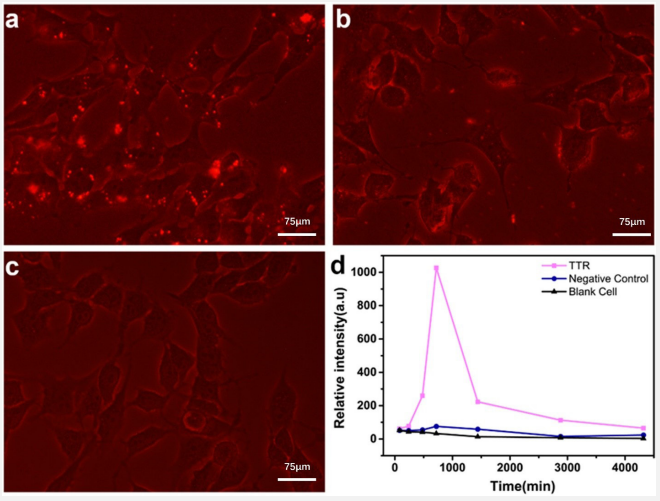

Figure 3: Fluorescent imaging of cellular transfection of TTR siRNA. Fluorescence images at the 12th hour after cellular transfection of TTR-siRNA **(A)** or NC-siRNA **(B)** molecular probes, which were compared with blank cells **(C)**. **(D)** Fluorescence intensity-time curves of TTR-siRNA- and NC-siRNA-treated groups, and the Blank Cell (BC) group.
Abbreviation: TTR: Transthyretin; siRNA: Small Interfering RNA; NC: Negative Control; BC: Blank Cell.

Figure 4: Western blot analysis for targeting of TTR-siRNA molecular probe to TTR mRNA. TTR-siRNA and NC-siRNA with N-TER as the vector were transfected into normal rat liver cells at 40 nM for 48 h. Western blots detected TTR protein expression, and TTR in the Blank Cell (BC) group was the control. β-actin was used as the housekeeping protein.
Abbreviation: TTR: Transthyretin; siRNA: Small Interfering RNA; NC: Negative Control; BC: Blank Cell.

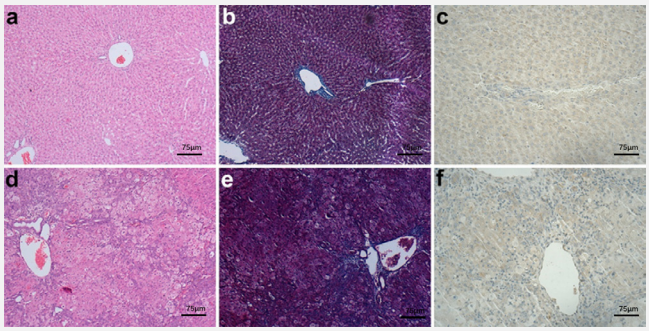

Figure 5: Pathological results of rat liver. **(A-C)** HE, Masson and TTR protein staining of rat tissues in the healthy group. **(D-F)** HE, Masson and TTR protein staining of rat tissues in the liver fibrosis-model group.
Abbreviation: TTR: Transthyretin; HE: Hematoxylin-Eosin.

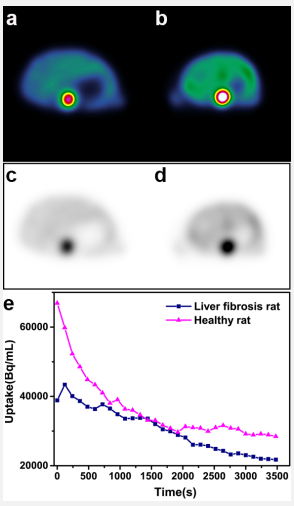

Figure 6: Uptake of [^{18}F] TTR-siRNA molecular probe by livers of rats in the healthy and liver fibrosis-model groups. **(A,C)** Pseudocolor and grey scale PET imaging of probe accumulation at 60 min after injection of molecular probe into rats in the liver fibrosis-model group. **(B,D)** Pseudocolor and grey scale PET imaging of probe accumulation at 60 min after injection of molecular probe into rats in the healthy group. **(C)** Radioactivity time curves of molecular probe in the livers in the liver fibrosis and healthy groups.
Abbreviation: TTR: Transthyretin; siRNA: Small Interfering RNA.

Discussion

In this study, siRNA targeting a specific sequence of TTR mRNA was used as a biomarker of liver fibrosis. The potency and feasibility of liver fibrosis imaging and diagnosis using the synthetic TTR-siRNA molecular probe was evaluated in vitro and in vivo.

We reached the following conclusions from cellular experiments: First, we achieved high-efficiency transmembrane delivery of siRNA by noncovalent binding of commercial transmembrane peptide nanoparticles N-TER to the siRNA. This result met the initial requirements of gene imaging. Second, cellular fluorescence imaging showed that the TTR siRNA combined with N-TER accumulated in the cytosol at 80 min after transfection, peaking at 12 h post transfection. These results indicated a successful cytoplasmic transfection for the N-TER transfection system and provided a time frame reference for subsequent imaging experiments *in vivo*. Fluorescence imaging studies and western blots to study TTR gene silencing demonstrated that TTR siRNA showed targeting specificity to TTR mRNA. The results were in contrast to results with the negative control siRNA that showed low fluorescence intensity after transfection and little, if any, gene silencing effects. Targeted imaging of lesions expressing target genes can be achieved using specific siRNA-labeled imaging probes highly specific to the target gene [29,30]. After continuous incubation for 72 h without culture media changes, transfected cells did not show observable abnormalities by microscopy. This result suggested that the transfection system was basically safe at cellular level. These cellular studies provided a basis for TTR imaging in vivo.

Targeted imaging of lesions expressing target genes can be achieved using specific siRNA-labeled imaging probes highly specific to the target gene [29,30]. The [^{18}F] TTR-siRNA molecular probe was prepared by labeling N-TER with the positron nuclide ^{18}F. PET/CT imaging was performed with normal rats and liver fibrosis model rats. In the current study, the normal and liver fibrosis rats were chosen for comparison because there existed significant difference of TTR transcript level between them [28]. Hence, the characterizations for normal rat hepatic cells could be reasonably referred and the TTR mRNA targeting effect of the tracer could be well distinguished between the two groups. The radioactivity-time curve indicated that after injection of the molecular probe, liver signals were transiently elevated due to blood perfusion. Rats with liver fibrosis had reduced portal blood flow due to increased portal pressure and blood-flow radioactivity distribution was lower than in normal rats. Liver uptake of the radiotracer in both normal and fibrosis-model rats decreased gradually. The liver radioactivity distributions were similar for the two groups at 24 min. However, the liver uptake of radiotracer was significantly higher in normal rats than in liver-fibrosis rats at 80 min. SUVmean and SUVmax showed significant differences. Differences in radiotracer accumulation in livers of normal and fibrotic rats were consistent with the results of cellular experiments and immunohistochemistry. Immunohistochemistry showed that liver fibrosis-model rats had S4 stage disease and TTR protein in liver fibrotic areas was lower than in normal rat liver tissue. In conjunction with TTR siRNA targeting in cellular experiments, these results explained why the molecular probe accumulated in normal rat livers at a delayed imaging time point. Therefore, the [^{18}F] TTR-siRNA molecular probe used in gene imaging reflected TTR mRNA in liver parenchyma and showed high value for diagnosis of liver fibrosis.

This study preliminarily evaluated targeting of a TTR-siRNA molecular probe to the TTR gene and the feasibility of an [^{18}F] TTR-siRNA molecular probe for PET imaging in cells and living animals. The molecular probe had potential for early diagnosis of genetic alteration of TTR-related diseases. However, the

study had several limitations. First, the experiments were designed to preliminarily explore the feasibility of an siRNA-based probe for diagnosis of liver fibrosis. As for limited NTER reagent, the experiments had a limited number of imaged animal samples (one for each group). In addition, rats with S4 stage fibrosis were used to better understand the feasibility of the TTR-siRNA molecular probe for TTR-mRNA-targeted imaging *in vivo*. The TTR expression level and differentiation of TTR-siRNA probes in imaging liver fibrosis with different stages requires further study to achieve deeper insight for the probe's clinical value. The effectiveness of TTR-siRNA imaging probe for staging liver fibrosis could also be compared with inflammation indicator such as translocator protein (18 kDa)-TSPO probes [31]. Second, although the probe accumulation at TTR gene became obvious at 80 min after injection, the PET imaging time was still short and long-term metabolic conditions and clearance of the molecular probe in the liver were not observed. Biodistribution studies were not carried out in rats. Moreover, the labeling position of the positron nuclides needs to be optimized. In this study, the ^{18}F was mainly on the polypeptide of the transmembrane carrier, which could affect the targeted imaging. In future studies, siRNA could be directly labeled with ^{18}F nuclides, and the imaging effects of the two labeling strategies could be compared. In addition, the diagnostic value of the TTR-siRNA molecular probe as a PET tracer for early-stage liver fibrosis and the probe biodistribution will be focused on in future work, which could provide scientific support for further clinical translation.

Conclusion

A [^{18}F] TTR-siRNA molecular probe targeting TTR mRNA in the cytoplasm was synthesized and preliminarily validated *in vitro* and *in vivo*. Because TTR expression is closely related to liver fibrosis progression, this probe might have the potential to achieve noninvasive, molecular-targeted gene imaging of liver fibrosis staging to improve diagnosis, which is critical for precision therapy and real-time monitoring of liver cancer.

Abbreviations: TTR: Transthyretin; siRNA: small interfering RNA; PET: positron emission computed tomography; ^{18}F: Fluorine-18: CT: Computed Tomography; MRI: Magnetic Resonance Imaging; ASGPR: Asialogly Coprotein Receptor; mRNA: messenger RNA; Cy3: Cyanine-3; [^{18}F] FB: ^{18}F-Fluorobenzaldehyde; HE: Hematoxylin-Eosin; SUV: Standardized Uptake Value.

Declarations

Author contributions: Kong FL designed the research and contributed new probe design/synthesis or analytic tools; Shi YL provided conception and the fund of this research; Li Dai performed the research, analyzed the data and wrote the paper; Guo QY analyzed the data and revised the manuscript.

Funding: Supported by Natural Science Foundation of Shandong Province (ZR2023QH485 and ZR2023QH328).

Ethical statement: This study was approved by The Animal Care and Use committee of Qilu Hospital of Shandong University.

Conflict of interest: The authors declare that they do not have any affiliation with or financial relationship/interest in a commercial organization that could pose a conflict of interest.

References

1. Novo E, Cannito S, Paternostro C, Bocca C, Miglietta A, et al. Cellular and molecular mechanisms in liver fibrogenesis. Archives of Biochemistry & Biophysics. 2014; 548: 20-37.
2. Ramachandran P, Iredale JP Liver fibrosis: A bidirectional model of fibrogenesis and resolution. Qjm Monthly Journal of the Association of Physicians. 2012; 105: 813-817.
3. Ariane Mallat SL Cellular Mechanisms of Tissue Fibrosis. 5. Novel insights into liver fibrosis. Am J Physiol Cell Physiol. 2013; 305: 789-799.
4. Ahmad W, Ijaz B, Gull S, et al. A brief review on molecular, genetic and imaging techniques for HCV fibrosis evaluation. Virology Journal. 2011; 8: 53-68.
5. Yu S, Qiyong G, Fei X, et al. MR elastography for the assessment of hepatic fibrosis in patients with chronic hepatitis B infection: does histologic necroinflammation influence the measurement of hepatic stiffness? Radiology. 2014; 273: 88-98.
6. Yu S, Qiyong G, Fei X, Jiaxing S, Yuying G Short- and midterm repeatability of magnetic resonance elastography in healthy volunteers at 3.0 T. Magnetic Resonance Imaging. 2014; 32: 665-670.
7. Zhang X, Xin J, Shi Y, et al. Assessing activation of hepatic stellate cells by (99m) Tc-3PRGD2 scintigraphy targeting integrin αvβ3: a feasibility study. Nuclear Medicine & Biology. 2015; 42: 250-255.
8. Shi Y, Xia F, Li Q, et al. Magnetic Resonance Elastography for the Evaluation of Liver Fibrosis in Chronic Hepatitis B and C by Using Both Gradient-Recalled Echo and Spin-Echo Echo Planar Imaging: A Prospective Study. American Journal of Gastroenterology. 2016; 111: 823-833.
9. Jiménez CC, Sehgal A, Popov Y, et al. Specific hepatic delivery of procollagen α1(I) small interfering RNA in lipid-like nanoparticles resolves liver fibrosis. Hepatology. 2015; 62: 1285-1297.
10. Schnabl B, Farshchi-Heydari S, Loomba R, et al. Staging of fibrosis in experimental non-alcoholic steatohepatitis by quantitative molecular imaging in rat models. Nuclear Medicine & Biology. 2016; 43: 179-187.
11. Zhu B, Wei L, Rotile N, et al. Combined magnetic resonance elastography and collagen molecular magnetic resonance imaging accurately stage liver fibrosis in a rat model. Hepatology. 2016; 65: 1015-1025.
12. Chow AM, Mingqian T, Gao DS, et al. Molecular MRI of liver fibrosis by a peptide-targeted contrast agent in an experimental mouse model. Investigative Radiology. 2013; 48: 46-54.
13. Jan P, Brown DM, Masanobu K, et al. Peptides selected for binding to clotted plasma accumulate in tumor stroma and wounds. Proceedings of the National Academy of Sciences of the United States of America. 2006; 103: 2800-2804.
14. Hatori A, Yui J, Xie L, et al. Utility of Translocator Protein (18 kDa) as a Molecular Imaging Biomarker to Monitor the Progression of Liver Fibrosis. Scientific Reports. 2015; 5: 17327-17335.
15. Wang QB, Han Y, Jiang TT, et al. MR Imaging of activated hepatic stellate cells in liver injured by CCl of rats with integrin-targeted ultrasmall superparamagnetic iron oxide. European Radiology. 2011; 21: 1016-1025.
16. Hao-Wen K, Chuan-Lin C, Wen-Yi C, et al. (18)F-FBHGal for asialoglycoprotein receptor imaging in a hepatic fibrosis mouse model. Bioorg Med Chem. 2013; 21: 912-921.
17. Zhang D, Zhuang R, Guo Z, et al. Desmin- and vimentin-mediated hepatic stellate cell-targeting radiotracer99mTc-GlcNAc-PEI for liver fibrosis imaging with SPECT. Theranostics. 2018; 8: 1340-1349.
18. Maepa MB, Ely A, Arbuthnot P How successful has targeted RNA interference for hepatic fibrosis been? Expert Opinion on

Biological Therapy. 2017; 18: 1-8.

19. Bangen J-M, Hammerich L, Sonntag R, et al. Targeting CCl4-induced liver fibrosis by RNA interference–mediated inhibition of cyclin E1 in mice. Hepatology. 2017; 66: 1242-1257.

20. Liu C-H, Chan K-M, Chiang T, et al. Dual-Functional Nanoparticles Targeting CXCR4 and Delivering Antiangiogenic siRNA Ameliorate Liver Fibrosis. Molecular Pharmaceutics. 2016; 13: 2253-2262.

21. Marimani MD, Ely A, Buff MCR, et al. Inhibition of replication of hepatitis B virus in transgenic mice following administration of hepatotropic lipoplexes containing guanidinopropyl-modified siRNAs. Journal of Controlled Release. 2015; 209: 198-206.

22. Grimm D Small silencing RNAs: State-of-the-art. Adv Drug Deliv Rev. 2009; 61: 672-703.

23. Hatanaka K, Asai T, Koide H, et al. Development of Double-Stranded siRNA Labeling Method Using Positron Emitter and Its In Vivo Trafficking Analyzed by Positron Emission Tomography. Bioconjugate Chemistry. 2010; 21: 756-763.

24. Mercier F, Paris J, Kaisin G, et al. General method for labeling siRNA by click chemistry with fluorine-18 for the purpose of PET imaging. Bioconjugate Chemistry. 2011; 22: 108-114.

25. Mudd SR, Trubetskoy VS, Blokhin AV Hybrid PET/CT for Noninvasive Pharmacokinetic Evaluation of Dynamic PolyConjugates, a Synthetic siRNA Delivery System. Bioconjugate Chemistry. 2010; 21: 1183-1189.

26. Bartlett DW, Helen S, Hildebrandt IJ, Weber WA, Davis ME. Impact of tumor-specific targeting on the biodistribution and efficacy of siRNA nanoparticles measured by multimodality in vivo imaging. Proceedings of the National Academy of Sciences of the United States of America. 2007; 104: 15549-15554.

27. Niemietz C, Chandhok G, Schmidt H. Therapeutic Oligonucleotides Targeting Liver Disease: TTR Amyloidosis. Molecules. 2015; 20: 17944-17975.

28. Frédérique C, Martine H, Odile G, et al. Novel serum markers of fibrosis progression for the follow-up of hepatitis C virus-infected patients. American Journal of Pathology. 2009; 175: 46-53.

29. Meng L, Fu WR, Chun Li Z, et al. Noninvasive imaging of human telomerase reverse transcriptase (hTERT) messenger RNA with 99mTc-radiolabeled antisense probes in malignant tumors. Journal of Nuclear Medicine. 2007; 48: 2028-2036.

30. Meng L, Fu WR, Ping Y, Chun Li Z, Gang CY. Molecular imaging and pharmacokinetics of (99m) Tc-hTERT antisense oligonucleotide as a potential tumor imaging probe. Journal of Labelled Compounds & Radiopharmaceuticals. 2014; 57: 97-101.

31. Hatori A, Yui J, Xie L, et al. Utility of Translocator Protein (18? Kad) as a Molecular Imaging Biomarker to Monitor the Progression of Liver Fibrosis[J]. Scientific Reports. 2015; 5: 17327.